both angular and temporal character of analyzed signal as time window $w_T(t)$ has a fixed time length yet is being shifted with equal angular instances. Therefore, Fourier transform over t will produce angle-synchronized short time Fourier transform (eq.3) that can be interpreted as a frequency-shifting filterbank for which each frequency component is observed in angle-fixed intervals.

The angular-temporal spectrum is calculated via following Matlab® code:

```
function
[stft,steps,f,t,do,SCMS,ord_ax]=Angular_Temporal_STFT(x,fs,fi,step,win)

%%%%%%%%%%%%%%%%%%%%%%%%%%%%%%%%%%%%%%%%%%%%%%%%%%%%%%%%%%%%

% Jacek K. Urbanek - 2014

% It is advised to use normalized version of signal x as an input
% [std_phi,mean_phi]=STD_PHI_JU(x,fs,speed,cycles);
% xn=(x-mean_phi)./std_phi;

% INPUT:
% x - input vibration signal
% fi [number of cycles * 2pi] - phase of the signal
(2*pi*cumsum(speed)/fs;)
% step[2pi] - angular step
% win[s] - length of temporal window

% OUTPUT:
% stft - angle-fixed short-time Fourier transform
% SCMC - angular-temporal spectrum
% steps [2pi] - angular increments
% t[s] - temporal increments
% do [samples/2pi] - angular-sampling frequency
% f[Hz] - temporal frequency axis
% ord_ax[1/2pi] - angular frequency axis

%%%%%%%%%%%%%%%%%%%%%%%%%%%%%%%%%%%%%%%%%%%%%%%%%%%%%%%%%%%%

x=x(:);
N=length(x);
fi=fi-fi(1); % <- we are allways starting the phase from 0
win=2*round(win*fs/2); % window is now in samples and is allways even
do=2*pi/step;

steps=0:step:fi(end);
```

```
steps_ind=zeros(1,length(steps));

    stft=zeros(win/2,length(steps));

    h=waitbar(0,'please wait...');

for i=1:length(steps)

    [temp,ind]=min(abs(fi-steps(i)));
    steps_ind(i)=ind;

if steps_ind(i)+win>N
    xi=x(steps_ind(i):end).*hanning(length(x(steps_ind(i):end)));
else
    xi=x(steps_ind(i):steps_ind(i)+win-1).*hanning(win);
end
    fft_xi=fft(xi,win)/(0.5*win);
    stft(:,i)=fft_xi(1:end/2);
    waitbar(i/length(steps),h);
end
close(h);

stft(isnan(stft)==1)=0;

df=fs/win;
f=linspace(df/2,fs/2-df/2,win/2);
t=(steps_ind-1)/fs;

SCMS=(abs(fft(abs(stft')))); % <- angular-temporal spectrum
SCMS=SCMS(1:end/2,:);
ord_ax=linspace(0,do/2,length(steps)/2);
```

where:

```
function [std_phi,mean_phi]=STD_PHI_JU(x,fs,phi)

% Jacek K. Urbanek - 2014
% phase locked localized standard deviation for angular window equal
to 2pi

% INPUT:
% x - original vibration signal
% fs - sampling frequency [Hz]
% phi - phase [2pi] (phi=2*pi*(cumsum(speed)/fs);)

% OUTPUT:
% std_phi - localized angle-fixed standard deviation
% mean-phi - localized angle-fixed mean
```

```
x=x(:)';
win=1;


[xr,do]=JU_resample_phase(x,phi,fs);

win=round(win*do);

xr=[zeros(1,win) xr zeros(1,win)];

xrf=conv(xr,ones(1,win)/win,'same');

xr_sq=xr.^2;

xr_sq_f=conv(xr_sq,ones(1,win)/win,'same');

std_phi_r=(sqrt(xr_sq_f-xrf.^2));

std_phi_r=std_phi_r(win+1:end-win+1);
xrf=xrf(win+1:end-win);

std_phi=JU_inv_resample_phase(std_phi_r,phi);

mean_phi=JU_inv_resample_phase(xrf,phi);

function [X_res,do,fi2,t1,t2]=JU_resample_phase(x,ph,fs)

%OUTPUT
% X_res - resampled signal
% do - new sampling frequency (angular)

%INPUT
% x - original vibration signal
% ph - phase signal (in rads)
% fs - sampling frequency

ph=ph(:)';
x=x(:)';

ph=ph-ph(1);
N_rot=ph(end)/(2*pi);


N=length(x);
do=N/N_rot;

t1=(0:N-1)/fs;
```

```
fi2=linspace(ph(1),ph(end),N);
t2 = interp1(ph,t1,fi2,'spline');
X_res = interp1(t1,x,t2,'spline');


function [x]=JU_inv_resample_phase(xr,ph)

%OUTPUT
% x - signal in time domain


%INPUT
% xr - signal in angular domain
% ph - phase signal (in rads)
% fs - sampling frequency

ph=ph(:)';
xr=xr(:)';

ph=ph-ph(1);
N_rot=ph(end)/(2*pi);


N=length(xr);
do=N/N_rot;

fi2=linspace(ph(1),ph(end),N);

x=spline(fi2,xr,ph);
```

The proposed codes have been used to generate figures illustrated in chapter 4. Fig. 2 illustrates angular-temporal spectrum of a simulated signls, wheres fig. 3 illustrates angular-temporal spectrum of a real signal from the test bench used in the project realization.

4 Experiment Simulated signal example

To better explain the outcome of the proposed tool we used simulated signal as expressed by eq. 1. For simplicity we expressed amplitude of consecutive resonance

pulses A_n as a value proportional to the square of rotational speed. Each pulse was modelled as an exponentially descending sine wave of the frequency between 4 kHz and 6 kHz. Angle-fixed characteristic frequency of pulses is equal to 1 x $\dot{\varphi}(t)$ where $\varphi(t)$ denotes angular increments. Simulated rotational speed profile varied from 50 to 550 RPM and was chosen to mimic the run-up process. Resulting generated signal and corresponding rotational speed profile is presented in fig. 2.

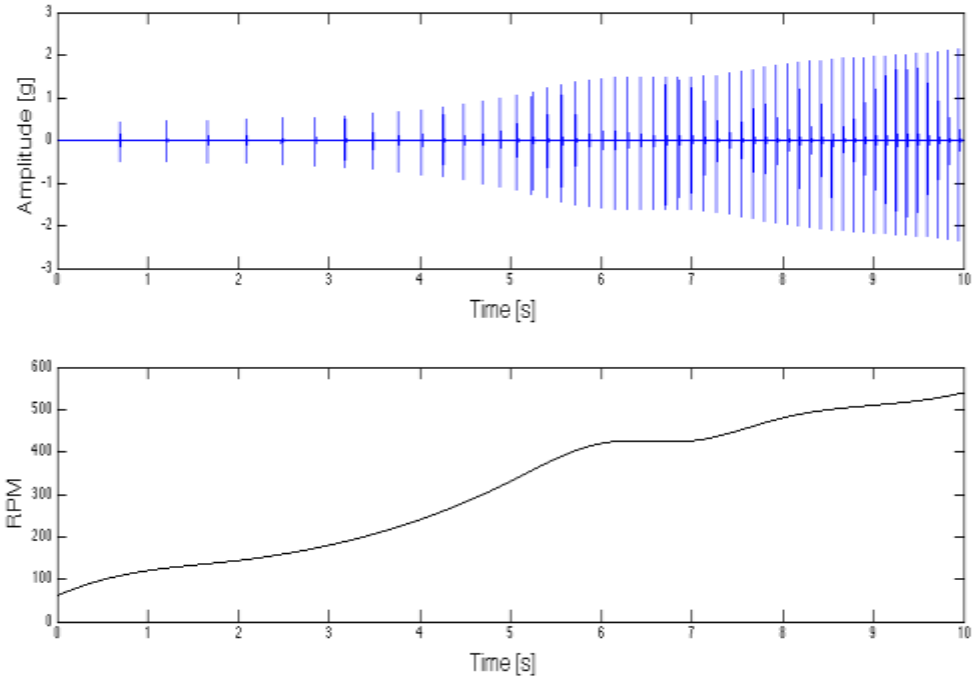

Fig. 2. Simulated signal used for presentation (top). Corresponding speed profile (bottom).

Angular-temporal spectrum calculated for the exemplary signal is presented in the fig. 3 as a colormap. Horizontal axis represents the frequency of angle-fixed cycles (Orders) of the analyzed signal while vertical axis represent frequency of time-fixed components. Therefore, vertical lines in the fig. 3 corresponds to phenomena

occurring cyclically once per each revolution (order No. 1); yet, exciting time-fixed components within the frequency range between 4 kHz and 6 kHz. Additionally, higher harmonics of angle-fixed components due to the overall shape of the each pulse.

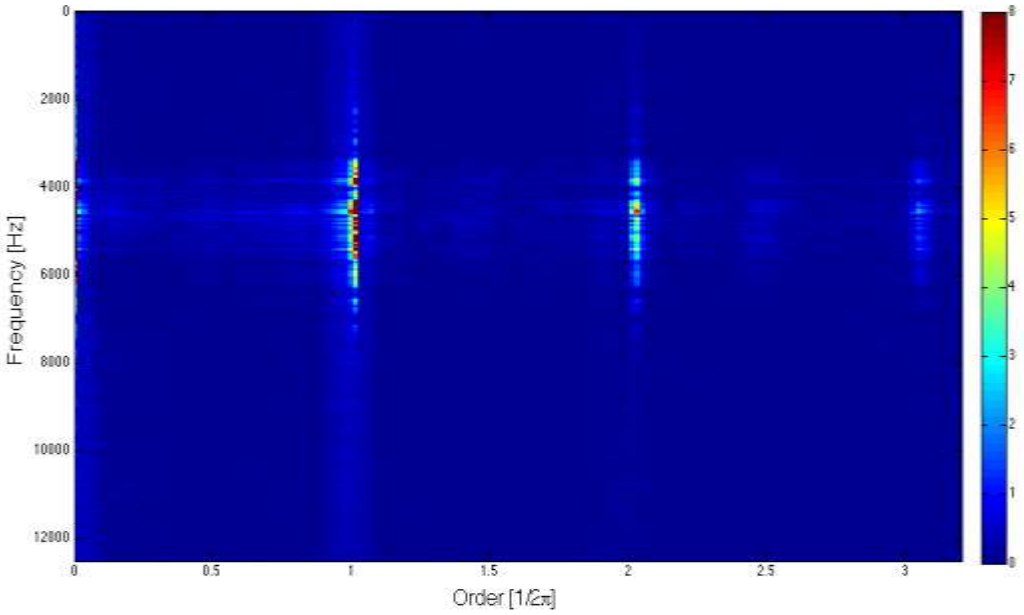

Fig. 3. Resulting angular-temporal spectrum of the simulated signal.

The magnitude of the resulting angular temporal spectrum is expressed in the units of the local standard deviation $\sigma_T(\varphi; \varphi_0)$. due to applied amplitude normalization.

5 Example Test-rig experiment

The test signals were collected from a test rig equipped with a 0,75 kW motor and 0,75 kW braking motor that introduced the load to the system, parallel gearbox with ratio 2.91, and two spherical rolling element bearings type YAR204-2F. The data was collected with the 4-channel NI card 9233, with sampling frequency 50 kHz and VIS-311B accelerometers with 30 kHz range. The motor and the braking unit were controlled by external software synchronized with the data collecting application, which enabled aquisition of vibration signals corresponding to a predefined speed and load profiles. Exemplary predefined speed profile is demonstrated in fig. 4. During this session, the load was held at a constant 0,33kW, and the torque was in range from 3Nm to 6 Nm.

Angular-temporal spectrum calculated for the test rig signal is presented in fig. 5. Horizontal lines located on order axis on the order no. 1 and its multiplicity correspond to main shaft rotational frequency. Additional component of angular-frequency equal to 5.1 is visible in the range of temporal-frequencies from 8 to 10 kHz (red arrow in fig. 5). That is the manifestation of the component related to damaged rolling element bearing where order of 5.1 corresponds to outer race characteristic frequency in relation to shafts rotational speed and the range of frequencies from 8 to 10 kHz represents the characteristics of machines' structural resonances excited by the damaged bearing. Additional components of 4.1 and 6.1 order are visible in fig.5 as well. Those are present due to amplitude modulations of bearing characteristic components with the component related to rotational speed and are artifacts of applied amplitude normalization.

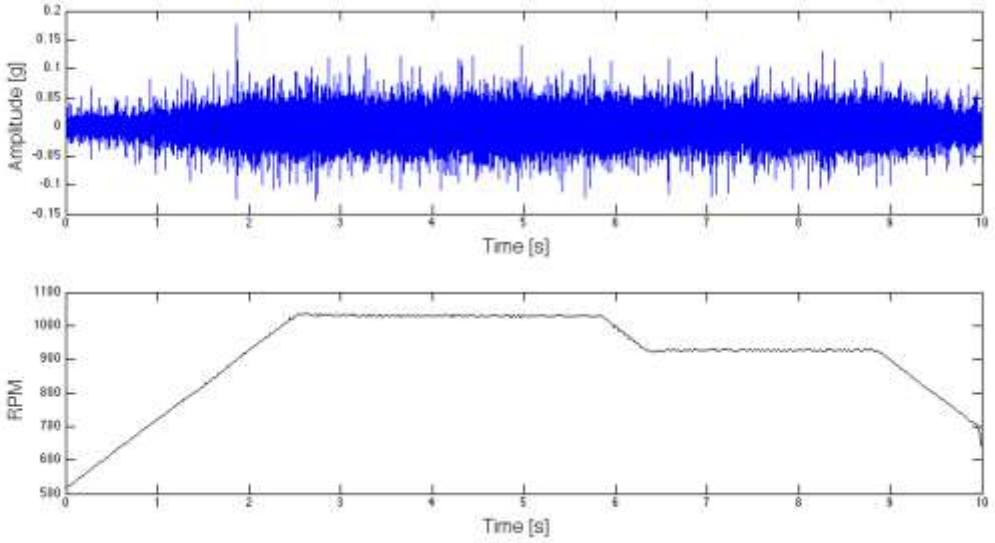

Fig. 4. A simulated test-rig speed profile and corresponding vibration signal

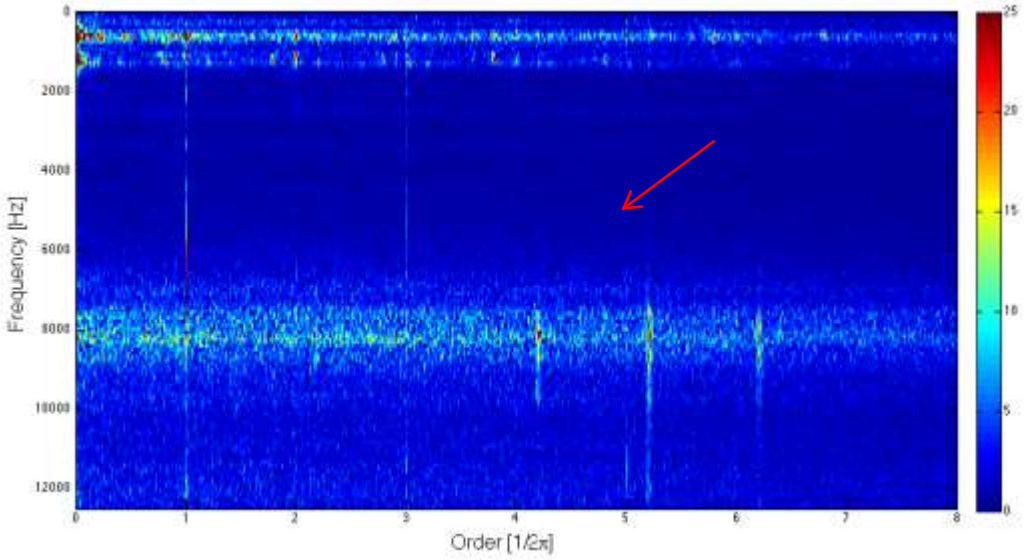

Fig. 5. Resulting angular-temporal spectrum applied to the simulated signal.

At this point, it is important to state that amplitude modulation of bearing characteristic signal is always present when dealing with inner race faults. However, it is not the case in the given example, and distinction between inner and outer race fault related components should be made based on their characteristic frequencies when using angular-temporal spectrum.

6 Conclusions

Angular-temporal spectrum allows to represent the signal in bi-frequency plane while preserving both; angular and temporal properties. As presented in given example angle-fixed characteristic even when rotational speed varies extremely during signal acquisition, it is still possible to identify characteristic frequencies of REB fault originated components as well as the range of excited resonances. Additionally, magnitude of angular-temporal spectrum is intuitive as it corresponds to the standard deviation of observed components within short-time window of analysis despite variations of their instantaneous amplitudes. The outcome of presented method depends on two tuning parameters namely synchronization phase φ_0 and window length T. Influence of those 2 parameters will be discussed in the follow-up of this paper

Acknowledgements

This work is supported by Polish Ministry of Science and Higher Education under research grant No. IP2012 061572.

7 References

1. Randall R.B.: Vibration-based condition monitoring, John Wiley & Sons, Ltd. (2011)
2. Antoni, J.: Cyclostationary by examples. Mech. Syst. and Sign. Proc. 23, 987–1036 (2009)
3. Bartelmus W., Zimroz R.: Vibration condition monitoring of planetary gearbox under varying external load, Mech. Syst. and Sign. Proc. 23, 246–257 (2009)
4. Bartelmus, W., Chaari, F., Zimroz, R., Haddar, M.: Modelling of gearbox dynamics under time-varying nonstationary load for distributed fault detection and diagnosis, European Journal of Mechanics - A/Solids, 29/4, 637–646 (2010)
5. Combet, F, Zimroz, R, A new method for the estimation of the instantaneous speed relative fluctuation in a vibration signal based on the short time scale transform, Mech. Syst. and Sign. Proc. 23, 1382–1397 (2009)
6. Leclere, Q., Pruvost L., Parizet E.: Angular and temporal determinism of rotating machine signals: The diesel engine case, Mech. Syst. and Sign. Proc. 24, 2012–2020 (2010)
7. Antoni J., et. al.: Cyclostationary modelling of rotating machine vibration signals, Mech. Syst. and Sign. Proc. 18, 1285–1314 (2004)
8. Antoni J., Randall, R.B.: Unsupervised noise cancellation for vibration signals: part II – a novel frequency-domain algorithm, Mech. Syst. and Sign. Proc. 18, 103–117 (2004)